

# Modes selection in polymer mixtures undergoing phase separation by photochemical reactions

Qui Tran-Cong,<sup>a)</sup> Junji Kawai, and Kouichi Endoh  
*Department of Polymer Science and Engineering, Kyoto Institute of Technology,  
Matsugasaki, Kyoto 606, Japan*

(Received 17 July 1998; accepted for publication 20 December 1998)

Phase separation kinetics and morphology of binary polymer mixtures (A/B) in the presence of photochemical reactions were investigated by using phase-contrast optical microscopy combined with digital image analysis. The polymers were chemically designed in such a way that two types of chemical reactions, intermolecular photodimerization and intramolecular photoisomerization, of polymer segments can be induced and controlled by irradiation with ultraviolet light. Unlike the conventional case, the phase separation in the presence of these reactions is spontaneously frozen due to the suppression of the long-wavelength instabilities, resulting in stationary spatial structures with intrinsic periodicities. These characteristic length scales are determined by the competition between the two antagonistic interactions: phase separation as a relatively short-range activation and the photochemical reaction as a long-range inhibition. Furthermore, it was found that the spatial symmetry breaking of concentration fluctuations can emerge from the elastic stress associated with the nonhomogeneous kinetics of the reactions. Experimental data obtained with three types of reactions: A-A only cross-link, A-A and B-B simultaneous cross-links and the reversible  $A \rightleftharpoons B$  photoisomerization are described. These results do not only indicate that combination of chemical reactions and phase separation could provide a novel method to control the morphology of multiphase polymer materials, but also suggest that photoreactive polymers can be used as a chemical system to study the mode-selection process in polymers far from thermodynamic equilibrium. © 1999 American Institute of Physics. [S1054-1500(99)00302-X]

In the past decades, the fact that physical properties of alloys are dictated by their phase-separated structures has promoted a large number of studies on morphology control from both fundamental and practical viewpoints. The so-called square gradient theory of Cahn and Hilliard has provided a concrete basis for the understanding of phase separation kinetics without chemical reactions. Here, the concentration fluctuations which grow fastest among others determine the final morphology. On the other hand, the phase separation of mixtures accompanied by chemical reactions is completely different from the case of nonreactive mixtures. In the presence of reversible and/or cross-linking reactions, phase separation can only proceed to some certain extent and eventually exhibits spontaneous pinning, giving modulated structures with various characteristic length scales. With light as a control parameter, photochemical reactions can be used as a tool for controlling not only the characteristic length scale, but also the spatial symmetry of the morphology by taking advantage of linearly polarized light. Unlike small molecule systems, the effects of changes in elasticity associated with chemical reactions in polymers contribute to the phase separation as a long-range interaction. These results suggest two possibilities: (1) polymer mixtures undergoing phase separation driven by chemical reactions can be used as a system to study the mode-selection process in media where elasticity has a

pronounced role; (2) polymeric materials with novel morphologies can be obtained by coupling chemical reactions with phase separation. Finally, these experimental data might provide useful information for modeling of reaction-diffusion with long-range elasticity.

## I. INTRODUCTION

Polymers that are composed of chainlike molecules are often immiscible with each other because the mixing entropy greatly decreases with increasing the chain lengths and, in most cases, their specific interactions are unfavorable for miscibility at molecular scale.<sup>1</sup> Besides these thermodynamical reasons, the fact that the gaps between the glass transition and the decomposition temperatures are relatively narrow for most polymers is also responsible for the immiscibility of polymer mixtures. Therefore, for most cases, polymer mixtures undergo phase separation upon mixing, giving multiphase polymeric materials. Similar to metallic alloys, extensive research on multiphase polymers in the past three decades has shown that the physical properties such as viscoelastic, optical, thermal, and mechanical properties of polymer blends critically depend on their phase-separated structures.<sup>2</sup> For the purpose of improving polymer functionality, morphology control has been one of the long-standing research subjects in practical as well as fundamental polymer science.

Over the past decades, a wide variety of techniques has been developed to improve the morphology control of multiphase polymeric materials. From the chemical viewpoint,

<sup>a)</sup>Corresponding author. Electronic mail: qui@ipc.kit.ac.jp

sophisticated polymerization techniques such as living anionic polymerization<sup>3</sup> were discovered and intensively developed to synthesize homopolymers with narrow molecular weight distribution and block copolymers with well-defined chemical structures.<sup>4</sup> Though polymer solids with a large number of ordered structures such as hexagon, lamella, gyroids and so on can be obtained with this particular polymerization method, their characteristic length scales are restricted in the nanometer scale due to the limitation of the polymerization mechanism. Alternatively, morphology in the micrometer range of multiphase polymers can be also controlled by the physical methods such as mechanical stirring<sup>5</sup> or applying a shear field<sup>6</sup> to polymer mixtures. Though the length scales of these structures can be regulated to some certain extent, it is not able to control the regularity of the morphology by using these physical methods. Therefore, it would be of great benefit for polymer materials science if some novel methods can be developed to control both the regularity as well as the characteristic length scales of the morphology ranging from nanometer to micrometer. One of the useful approaches would be applying the principle of nonlinear dynamics to systems far from equilibrium<sup>7,8</sup> to generate and control the spatio-temporal structures of polymer materials. Particularly, materials processing, in reality, is carried out under nonequilibrium conditions. In metallurgy, unique phenomena such as directional solidification<sup>9</sup> or phase ordering of metallic alloys bombarded with high-energy particles<sup>10</sup> have been observed under thermodynamical nonequilibrium conditions. These experimental data have been analyzed in terms of reaction-diffusion mechanism.<sup>11</sup>

In this paper, we show that photochemical reactions can be used as a useful tool to generate and control the length scale as well as the symmetry of modulated structures in polymer mixtures by taking advantages of the competition between the reactions and the phase separation. Here, two types of photochemical reactions: photodimerization of anthracene and *trans*-cinnamic acid [Figs. 1(a) and 1(b)], and photoisomerization of stilbene [Fig. 1(c)] were used as the typical reactions for these purposes. The first two reactions initiate the cross-link between different segments of polymer chains, leading to the network formation whereas the third one is an intramolecular reaction initiating phase separation by the changes in volumes as well as in dipole moments of the *trans*- and *cis*-isomers. Figure 2 schematically shows the reactions in binary polymer mixtures under irradiation for these three cases. Unlike thermally activated reactions, photochemical reactions can be initiated and terminated independently from thermodynamic variables such as pressure and temperature, thus providing an efficient way for the morphology control.

First, the recent analytical theories of phase separation with and without chemical reactions are briefly reviewed. The phase separation kinetics and the morphology of polymer blends obtained by the A-A only cross-link reaction inside the spinodal as well as in the one-phase regions, and subsequently by the A-A, B-B simultaneous cross-links in the miscible region, are discussed in conjunction with the mechanism of freezing the long-wavelength fluctuations, i.e., the so-called soft modes, predicted by theories. Suppression

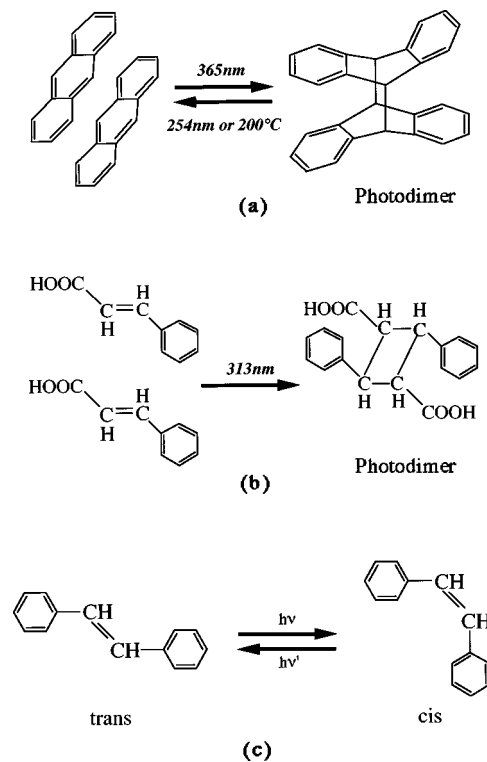


FIG. 1. Photochemical reactions used to induce phase separation of polymer mixtures: photodimerization of anthracene (a) and of *trans*-cinnamic acid (b); photoisomerization of stilbene (c).

of these modes in polymer blends in the presence of the reversible photoisomerization  $A \rightleftharpoons B$  was also experimentally investigated. The mathematical analogy between the phase separation of binary polymer blends accompanied by reversible chemical reactions and the microphase separation of diblock copolymers was experimentally examined with emphasis on the role of elastic stress arising from the nonhomogeneous reaction kinetics. The perspectives of controlling morphology via the selection process of unstable modes by using chemical reactions in polymers are finally discussed.

## II. THEORETICAL BACKGROUND OF PHASE SEPARATION IN BINARY POLYMER MIXTURES

### A. Phase behavior of polymer mixtures

Similar to small-molecule systems, the miscibility of a binary polymer mixture (A/B) is determined by the change in the Gibbs free-energy associated with the mixing process:

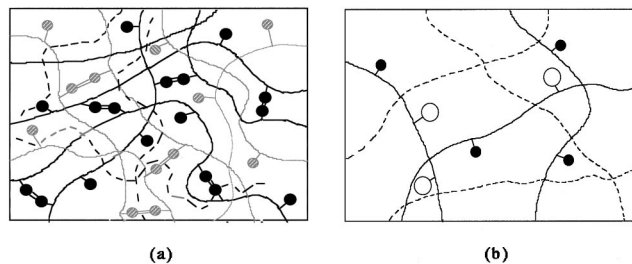


FIG. 2. Schematic presentation of polymer reactions in polymer mixtures. (a) A-A only, A-A and B-B simultaneous cross-links: (●), anthracene; (○), the corresponding photodimer; (○), unreacted cinnamic acid ester; (○=○), the corresponding photodimer (b)  $A \rightleftharpoons B$  photoisomerization: (●), *trans*-stilbene; (○), *cis*-stilbene. (---): unreacted chains.

$$\Delta F = \Delta H - T\Delta S. \quad (1)$$

Here,  $F$ ,  $H$ , and  $S$  are the Gibbs free-energy, enthalpy and entropy, respectively. Generally, compared to small molecules, polymers are not easily miscible with each other due to the small change in mixing entropy. The first thermodynamical theory of polymer mixtures, known as the mean-field theory, was formulated by Flory and Huggins.<sup>12</sup> This becomes a basis for the theoretical description of polymer miscibility. Polymer mixtures can possess an upper critical solution temperature (UCST) and/or a lower critical solution temperature (LCST). The latter behavior is the characteristic feature of polymeric systems, arising from the mismatch in free-volumes between polymer components. There exists a number of polymer mixtures that are miscible at ambient temperature and undergo phase separation upon increasing temperature like the mixtures of poly(vinyl methyl ether) and polystyrene derivatives discussed below.

## B. Phase separation kinetics of polymer mixtures

### 1. Nonreactive mixtures

Phase separation kinetics of polymer mixtures was formulated by extending the Cahn-Hilliard linearized theory<sup>13,14</sup> for metallic alloys to polymers using the Flory-Huggins mean-field free-energy.<sup>15</sup> For the case of a nonreactive binary mixture (A/B), the time evolution of the composition  $\phi$  of one polymer component can be written in terms of its flux  $J$  with respect to the other component:

$$\frac{\partial \phi}{\partial t} = -\nabla J \quad (2)$$

and

$$J = -M\nabla\mu,$$

where  $M$  is the mutual mobility of A and B, and  $\mu = (\mu_2 - \mu_1)$  is the difference in the chemical potential between the two polymer components.

By substituting  $\mu = \delta F / \delta \phi$  into (2), the equation of motion can be rewritten in terms of functional derivative of free-energy:

$$\frac{\partial \phi}{\partial t} = M\nabla^2 \frac{\delta F}{\delta \phi}. \quad (3)$$

In Eq. (3)  $F$  is the Cahn-Hilliard free-energy:

$$F(\phi) = \int dr [f(\phi) + \kappa(\nabla\phi)^2]. \quad (4)$$

Here  $f(\phi)$  is the free-energy of the mixture in a homogeneous state taken as the Flory-Huggins free-energy for polymeric systems. The second term on the rhs of (4) is the square-gradient term coming from fluctuations. The coefficient  $\kappa$  expresses the strength of the interactions between the two components. After linearization with respect to the average composition  $\phi_0$ , the equation of motion for the fluctuations in composition  $\delta\phi = (\phi - \phi_0)$  is

$$\frac{\partial(\delta\phi)}{\partial t} = M\nabla^2 \left[ \left( \frac{\partial^2 f}{\partial \phi^2} \right) (\delta\phi) - 2\kappa\nabla^2(\delta\phi) \right]. \quad (5)$$

The solution of (5) in Fourier space is obtained by the conventional way:

$$\delta\phi_F(q, t) = \delta\phi_F(q, 0)e^{R(q)t}, \quad (6)$$

predicting that the growth rate  $R(q)$  of the fluctuation with the wave number  $q$  is

$$R(q) = Mq^2 \left[ - \left( \frac{\partial^2 f}{\partial \phi^2} \right) - 2\kappa q^2 \right]. \quad (7)$$

The dispersion relation (7) predicts that once the mixture are brought inside the immiscible region, all the unstable modes will grow until phase equilibrium with random two-phase structures is achieved. The mode with infinitive wavelength is metastable [ $R(q \rightarrow 0) = 0$ ].

### 2. Binary mixtures with reversible reactions

Studies on phase separation of a binary mixture A/B accompanied by the reversible reaction  $A \rightleftharpoons B$  were initiated recently by Glotzer and co-workers.<sup>16</sup> Analytical solutions for the linear region and numerical calculations for the late stage kinetics have been subsequently carried out by a number of research groups.<sup>17-19</sup> Recently, from a general viewpoint of nonequilibrium thermodynamics of reacting mixtures, Lefever and Carati have shown that, instead of Eq. (7), the dispersion relation in the presence of a reversible reaction is<sup>20</sup>

$$R(q) = N(\phi_0)Z(\phi_0) + [I(\phi_0, \delta) - Z(\phi_0)]q^2 - q^4. \quad (8)$$

Here  $N(\phi_0)$ , the reaction parameter, is determined by the forward and backward reaction kinetics and plays a crucial role in the stability of the reacting mixture,  $Z(\phi_0)$  is a nondimensionalized second derivative of free-energy of the mixture  $[\partial^2 f(\phi) / \partial \phi^2]_{\phi=\phi_0}$  and  $I(\phi_0, \delta)$  is the parameter determined by both the reaction kinetics and the ratio of the homo- to the hetero-interaction energies between the two components of the mixtures. Depending on the sign of  $N(\phi_0)$  and  $Z(\phi_0)$ , the following cases were identified:

- $Z(\phi_0) > 0$  and  $N(\phi_0) > 0$ : The mixture is miscible but can exhibit purely chemical instability due to the non-linearity of the reaction kinetics.
- $Z(\phi_0) > 0$  and  $N(\phi_0) < 0$ : The mixture is miscible but is able to exhibit the Turing-like instability<sup>7,8</sup> due to the large difference between the homo-interactions of the two components in the mixture.
- $Z(\phi_0) < 0$  and  $N(\phi_0) < 0$ : The mixture is thermodynamically unstable. This case is equivalent to the conventional spinodal decomposition process as in the absence of the reaction.
- $Z(\phi_0) < 0$  and  $N(\phi_0) > 0$ : The mixture undergoes phase separation, leading to the suppression of the long-wavelength fluctuations (the soft modes). The stationary structure possesses intrinsic length scales determined by the competition between phase separation and the reaction as schematically shown in Fig. 3.

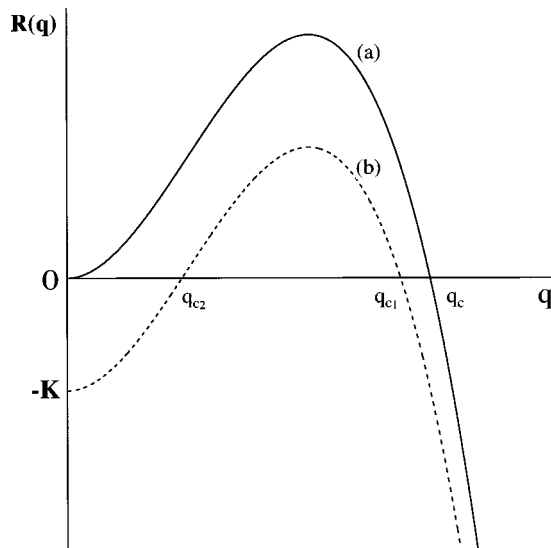


FIG. 3. Dispersion relation obtained from the linearization of the equation of motion for phase separation: (a) without chemical reaction; (b) in the presence of a reversible reaction.  $K$ : the constant determined by reaction kinetics.

### 3. Phase separation of binary polymer mixtures induced by photo-cross-linking reactions

For polymeric systems, the contribution of the viscoelasticity to the free-energy of the mixtures during the reaction becomes significant, making the problems complicated. Currently, there are no theories to explain satisfactorily the phenomena. Based on the experimental data of the spinodal decomposition process frozen by the photo-cross-linking reactions of the A-A type in binary polymer mixtures,<sup>21</sup> Nakazawa and Sekimoto recently propose a viscoelastic model for the phase separation of a mixture composed of a nonreactive polymer component trapped inside a network growing by photo-cross-linking reactions.<sup>22</sup> The equation of motion for the deformation  $\lambda$  of the mixture is

$$\frac{\partial \lambda}{\partial t} = \frac{\partial}{\partial X} \left[ \frac{\Gamma}{\lambda} \frac{\partial}{\partial X} \Pi \right], \quad (9)$$

where  $X$  is the coordinate in the homogeneous and thermodynamically stable cross-linked mixture (called gel), taken as a reference state. Here  $\Gamma$  is the Onsager transport coefficient. The volume fraction  $\phi(X)$  of the gel under a deformation  $\lambda$  is related to that of the homogeneous gel by  $\phi(X) = \phi_0/\lambda(X)$  where  $\phi_0$  is the volume fraction of the initial homogeneous cross-linked mixture. The free-energy of the mixture is composed of two parts, the osmotic  $F_{os}$  and the elastic free-energy  $F_{el}$ . The total free-energy  $F = F_{os} + F_{el}$  is thus related to the osmotic stress  $\Pi(X)$  of the reacting mixture by

$$\Pi(X) = \frac{\delta F}{\delta \lambda(X)} = \Pi_{os} + \Pi_{el}. \quad (10)$$

The Flory-Huggins free-energy is included in the osmotic part  $\Pi_{os}$ , and the viscoelastic part  $\Pi_{el}$  was assumed to contain a memory function recording the history of the cross-

TABLE I. Characteristics of polymers used to induce phase separation in this work.

Polymers	$M_w$	Label content <sup>a</sup>	Type of cross-link
P2CSA	$2.1 \times 10^5$	55	A-A only cross-kink
PSA	$2.7 \times 10^5$	40	A-A only cross-kink
PSC	$2.0 \times 10^5$	38	
PSA-2	$2.0 \times 10^5$	35	A-A and B-B simultaneous cross-link
PSS	$3.2 \times 10^5$	160	A $\rightleftharpoons$ B isomerization
PVME	$1.0 \times 10^5$	...	...

<sup>a</sup>Average number of labels per chain.

linking reaction. This function is related to the cross-link density  $\nu$  via the reaction kinetics by using the mean-field approximation:

$$\frac{d\nu}{dt} = K(\nu_\infty - \nu)^2, \quad (11)$$

where  $\nu$  and  $\nu_\infty$  are the cross-linking densities at a time  $t$  and  $t = t_\infty$ . Here, the reaction was assumed to proceed homogeneously with the rate constant  $K$  independent from the thermodynamics of the reacting mixture. Equation (11) models the photodimerization kinetics of anthracene labeled on one polymer component of the binary blends. By varying the reaction rate  $K$ , the reaction-time dependence of the deformation  $\lambda(X, t)$  and of the volume fraction  $\phi(x, t)$  were calculated. It was predicted that the phase separation was frozen as the cross-linking reaction reaches a critical value. Furthermore, the freezing effect is more effective for slower cross-linking reactions.

## III. EXPERIMENTAL SECTION

### A. Characteristics and chemical reactions of polymers

Samples used in this work are the three mixtures: anthracene-labeled polystyrene/poly(vinyl methyl ether) (PSA/PVME), cinnamic acid-labeled polystyrene/poly(vinyl methyl ether) (PSC/PVME) and *trans*-stilbene labeled polystyrene/poly(vinyl methyl ether) (PSS/PVME). To increase the contrast for optical microscopy and for small-angle x-ray scattering (SAXS) experiments, anthracene-labeled poly(2-chlorostyrene) (P2CSA) was also mixed with PVME. The phase separation behavior of P2CSA/PVME is, in general, similar to the PSA/PVME mixture. Except PVME purchased from Aldrich Chem. Co., all other polymers were synthesized according to the procedure described previously.<sup>21</sup> Three types of photochemical reactions are utilized to induce phase separation of binary polymer mixtures (A/B): A-A type cross-link via photodimerization of anthracene, A-A and B-B simultaneous cross-link by using photodimerization of both anthracene and cinnamic acid derivatives,<sup>23</sup> and the reversible photoisomerization of stilbene.<sup>24</sup> The characteristics and chemical structures of these photosensitive polymers are summarized in Table I together with their chemical structures illustrated in Fig. 4. The samples with the size ( $6 \times 12 \times 0.05$  mm<sup>3</sup>) are dried under vacuo over two nights at 60 °C. Subsequently, the mixtures

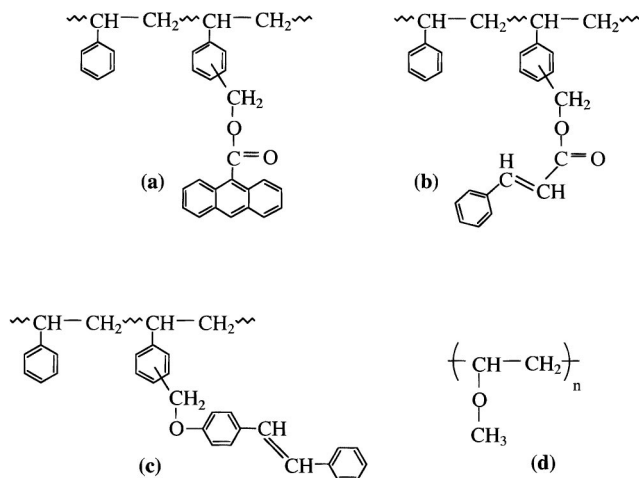


FIG. 4. Chemical structures of polymers used in this work: (a) PSA; (b) PSC; (c) PSS and (d) PVME.

are sandwiched between two glass plates with an aluminum spacer used to adjust the sample thickness prior to the experiments.

All the blends used in this work have a lower critical solution temperature (LCST). As an example, the phase diagram of a P2CSA/PVME blend is shown in Fig. 5 with both the coexistence curve and the spinodal line determined by small-angle x-ray scattering.<sup>21</sup>

## B. Irradiation experiments

Polymer mixtures were irradiated with ultraviolet light from a Hg–Xe lamp (500 W, Hamamatsu Photonics). The two lines at 313 and 365 nm were selected from the light source by using appropriate optical filters and subsequently focused at the sample kept in a brass heating block. The details of the optical arrangements were described elsewhere.<sup>25</sup> The intensity of the above two lines is variable

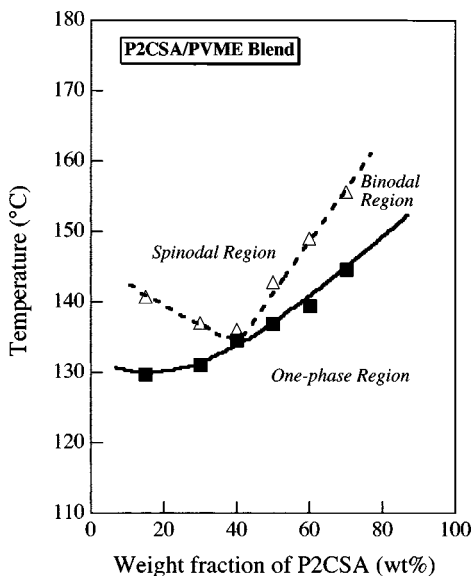


FIG. 5. Phase diagram of an anthracene-labeled poly (2-chlorostyrene)/poly (vinyl methyl ether) mixture determined by using small-angle x-ray scattering (SAXS).

in the range 0.1–7.0 mW/cm<sup>2</sup>. The temperature was thermostated with a precision of  $\pm 0.5^\circ\text{C}$  by using a temperature controller (Okura Electric, SC-5600).

## C. Morphological observation and data analysis

Morphology of these reacting mixtures was observed by using a phase-contrast optical microscope (Nikon, Model XTF-21). The images were digitalized by using an image analyzer (Pias, Model LA-525) and were then transferred to a computer (Macintosh 7100-80AV) where further structure analysis such as two-dimensional fast Fourier transform (2D-FFT) was performed by using standard softwares for image analysis such as Scion Image<sup>®</sup> and IP Lab Spectrum<sup>®</sup> (Signal Analytics Corp.). From the 2D-FFT power spectra data, the characteristic length scale  $\xi$  of the structures was obtained by using the Bragg formula:

$$\xi = \frac{2\pi}{q_{\max}}. \quad (12)$$

Here  $q_{\max}$  is the wave number corresponding to the maximum of the power spectra. To increase the S/N ratio,  $q_{\max}$  was obtained either from circular average of the isotropic or from sector average of the anisotropic power spectra.

## IV. EXPERIMENTAL RESULTS AND DISCUSSION

### A. Phase separation of binary polymer mixtures with the A-A type photo-cross-linking reactions

As described in Sec. II, a polymer mixture undergoes spinodal decomposition as soon as it was brought into the unstable region. In the initial stage, the wavelength of fluctuations is unchanged whereas their amplitude grows with time as predicted by the Cahn-Hilliard linearized theory.<sup>13</sup> Subsequently, these structures become more and more coarsened, and finally the mixture reaches phase equilibrium with random two-phase structures. The intermediate structures developing during the spinodal decomposition process of the P2CSA/PVME blend can be frozen by forming the P2CSA networks trapping PVME chains via photodimerization of anthracene. This freezing process can be observed with a P2CSA/PVME (60/40) blend irradiated over 30 min with 365 nm uv light after a temperature jump from 100 °C (the one-phase region) to 152 °C (the spinodal region). The quench depth, i.e., the distance from the spinodal line, is 2 °C for this particular case. The morphology of the blend observed by phase-contrast optical microscopy under this experimental condition is an interconnecting structure in the micrometer scale as revealed by the ‘‘ring-shaped’’ 2D-FFT power spectra. After cross-linking, the blend was annealed in the dark at the experimental temperature. The time evolution of the characteristic length scales  $\xi$  calculated from Eq. (12) is illustrated in Fig. 6. In the early stage,  $\xi$  grows with irradiation time to a certain extent and then tends to approach an equilibrium value, revealing the freezing process of the spinodal decomposition by the photo-cross-linking reaction. Similar phenomena was also observed with a PSA/PVME (50/50) blend photo-cross-linked in 35 min at 120 °C in the one-phase region located at 10.5 °C below the cloud point. Figure 7 shows the morphology of this particular blend under

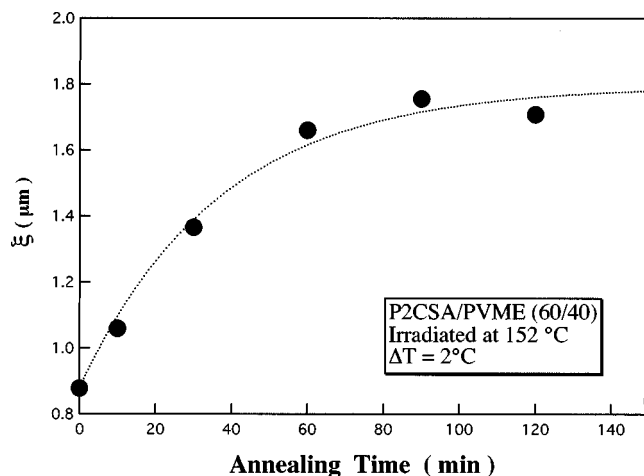


FIG. 6. Time evolution of the characteristic length scale of the morphology observed for a P2CSA/PVME (60/40) blend annealed at 152 °C in the dark after photo-cross-linked at the same temperature.

the irradiation condition. The corresponding “ring-shaped” 2D power spectra are shown in the inset of this figure, reflecting the interconnectivity of the morphology in the micrometer scale. The phase separation kinetics obtained by the reaction in the one-phase region is similar to the case of cross-link inside the spinodal region. This freezing process can be described by the scaling law proposed recently for binary mixtures undergoing phase separation in the presence of obstacles.<sup>26</sup> According to this prediction, the time evolution of the characteristic length scales  $\xi$  can be expressed by<sup>16</sup>

$$\xi(t) = t^\alpha G(x) \quad (13)$$

and

$$x = kt,$$

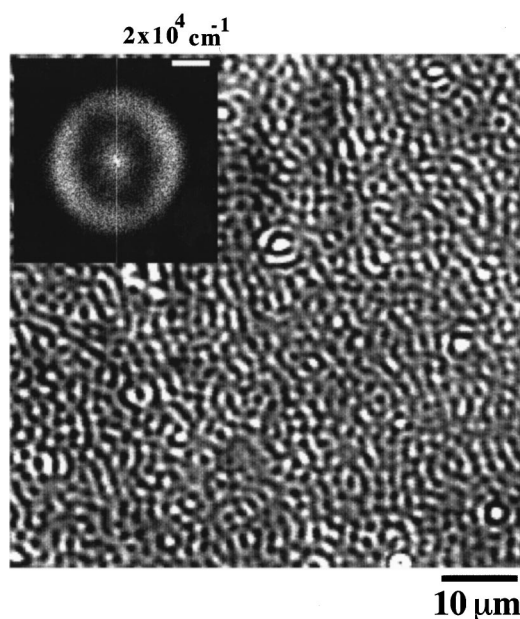


FIG. 7. Morphology and the corresponding 2D-FFT power spectra (the inset) of a PSA/PVME (20/80) blend photo-cross-linked with uv light at 365 nm over 35 min at 110 °C.

where  $k$  and  $t$  are the reaction rate and the reaction time, respectively. Here, the phase separation is assumed to evolve through two stages. In the early stage, the phase separation proceeds according to the power law  $t^\alpha$  without influence from the forming networks. As soon as the presence of the networks becomes effective, the phase separation is frozen. The scaling function  $G(x)$  has the following asymptotic behavior:

$$G(x) = \text{constant} \quad \text{for } x \ll \infty$$

and

$$G(x) \propto t^{-\alpha} \quad \text{for } x \rightarrow \infty \quad (14)$$

In order to test this scaling law, Eq. (13) is rewritten as

$$\xi(t)/t^\alpha = G(x). \quad (15)$$

Since the lhs of (15) can be directly determined by experiments, Eq. (13) can be experimentally justified by plotting  $\xi(t)/t^\alpha$  versus irradiation time. It was found that the scaling law given in (13) is in good agreement with the experimental data obtained for a PSA/PVME (20/80) blend photo-cross-linked at 110 °C as shown in Fig. 8. The exponent  $\alpha$  was found to be approximately  $\frac{1}{4}$  which corresponds to the weak segregation limit.

On the other hand, the photodimerization kinetics of anthracene obtained in the one-phase region far from the phase boundary of the PSA/PVME blends follows the Kohlrausch-Williams-Watts kinetics:<sup>27</sup>

$$OD(t) = (OD_0 - B) \exp(-k_0 t)^\beta + B, \quad (16)$$

indicating that the cross-linking reaction does not proceed homogeneously in the blend under irradiation. Here,  $k_0$  is the average reaction rate, and  $OD_0$ ,  $B$  and  $\beta$  are the initial absorbance of anthracene, the baseline and the inhomogeneity index. Here  $B$  was introduced into the kinetics to express the fact that the cross-linker anthracene is not always completely consumed under irradiation. An example is shown in Fig. 9 for a PSA/PVME (20/80) and a (50/50) blend photo-cross-linked respectively at 10 °C and 30 °C. It is worth noting that Eq. (16) does not hold at temperatures close to the phase boundary where the autocatalytic behavior of the cross-linking reaction was found recently.<sup>28</sup>

From the experimental results described above, we conclude that the A-A type of cross-linking reactions induced inside the spinodal as well as in the one-phase regions of binary polymer mixtures suppress the long-wavelength fluctuations in the reacting mixture. These experimental results suggest that morphologies with various intrinsic length scales can be obtained by appropriately adjusting the competition between the reaction and phase separation.

## B. Phase separation of binary polymer mixtures with A-A and B-B simultaneous photo-cross-linking reactions

In order to induce phase separation of polymer mixtures by the A-A and B-B simultaneous cross-link reactions, polystyrenes labeled with anthracene (PSA-2) and with a cinnamic acid derivative (PSC) were mixed with PVME to form tertiary blends (PSA-2/PSC/PVME) of various compositions.

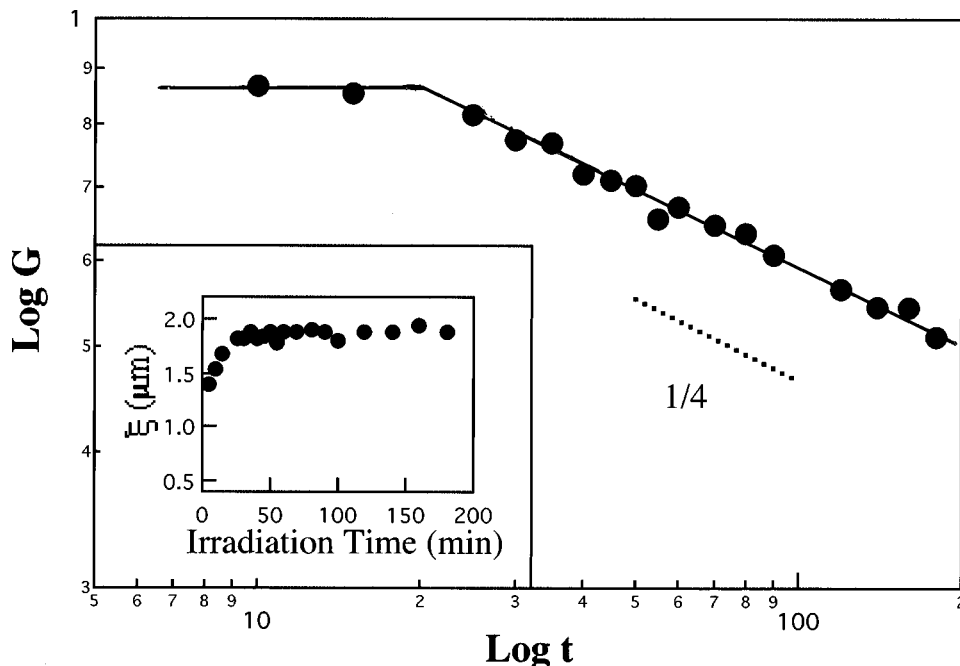


FIG. 8. Experimental verification for the scaling law given in Eq. (13). Inset: dependence of the length scale  $\xi$  on the irradiation time in real space.

The composition of the blend is varied in such a way that  $\phi_{\text{PSA}} = \phi_{\text{PSC}}$ . Upon irradiation with uv light at 313 and 365 nm, PSC and PSA-2 chain can be independently cross-linked in the ternary PSA-2/PSC/PVME blend. The reason for using the ternary system PSA-2/PSC/PVME instead of the binary PSA-2/PSC mixtures is that the latter is very brittle at ambient temperatures, resulting in some drawbacks in experiments using optical microscope and light scattering. Like other binary blends used in this work, the ternary PSA-2/PSC/PVME mixture possesses a lower critical solution temperature and undergoes phase separation upon cross-linking. The effects of the cross-linking reaction kinetics on the morphology of the blend were examined by carrying out two typical experiments. One is performing the simultaneous A-A (via photodimerization of anthracene) and B-B (via photodimerization of cinnamic acid derivatives) photo-cross-linking reactions by using two excitation wavelengths of 365

and 313 nm. The former wavelength is used to induce only the reaction of anthracene on the PSA-2 chains whereas the latter can simultaneously initiate the photodimerization of both the anthracene moieties on the PSA-2 chains and the cinnamic acid derivative on the PSC component. These results are then compared to the case of A-A only cross-linking obtained for the same blend. It should be noted that to facilitate the comparison, the cross-linking reaction kinetics of anthracene in both experiments were matched within 5% by adjusting the intensity of the excitation light. These photo-cross-linking conditions are summarized in Table II. Shown in Fig. 10(a) are the morphology and the corresponding 2D-FFT power spectra of a PSA-2/PSC/PVME (20/20/60) blend obtained by cross-link in the miscible region under the condition (2) indicated in Table II. Compared to the same blend with the A-A only cross-link obtained by photodimerization of anthracene at the same temperature under the condition (1), the blend with simultaneous A-A and B-B cross-links exhibits modulated morphology that is much more regular than the A-A only cross-linking reaction. This conclusion is based on the time evolution of the half-width at maximum of the 2D-FFT power spectra obtained for both cases. These experimental results imply that, compared to the A-A only cross-link type, the bandwidth of the wave numbers of the unstable modes (Fig. 3) involving in the phase separation of the PSA-2/PSC/PVME (20/20/60) blend was narrowed by the A-A and B-B simultaneous cross-linking reactions. In

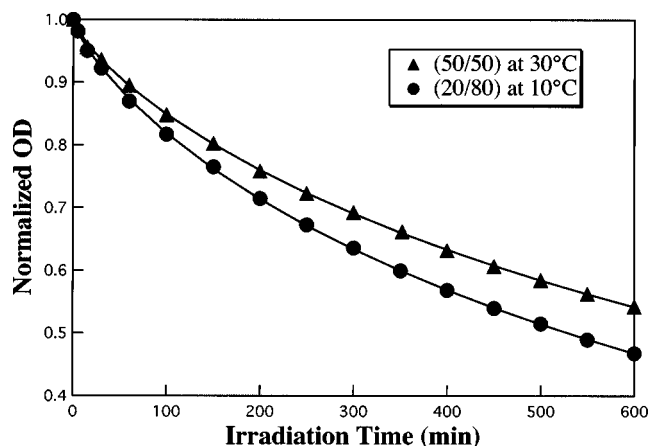


FIG. 9. Photo-cross-link kinetics of PSA/PVME (50/50) and (20/80) blends observed respectively at 30 °C and 10 °C by monitoring the absorbance of anthracene at 410 nm. The difference between the experimental temperature and the glass transition of these two blends is the same.

TABLE II. Photo-cross-linking conditions for the morphological results shown in Fig. 10.

Condition	Type of cross-links	Irradiation time (min)	Conversion (%)	Excitation (nm)
(1)	A-A	60	31	$\geq 360$
(2)	A-A	60	24	$\geq 290$
	B-B		3	

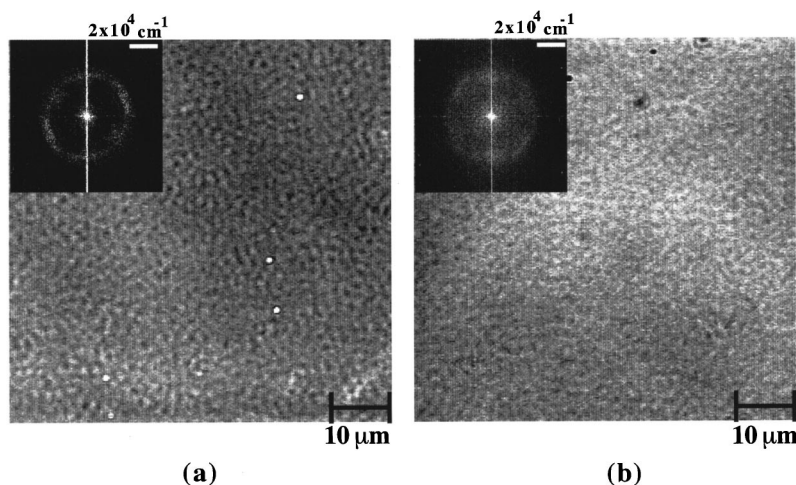


FIG. 10. Morphology and the corresponding 2D-FFT power spectra of a tertiary PSA-2/PSS/PVME (20/20/60) blend obtained by (a), A-A and B-B simultaneous photo-cross-link; (b) A-A only cross-link. The experimental conditions are summarized in Table II.

other words, the above results suggest that photo-cross-linking reactions do not only suppress the evolution of the long-wavelength fluctuations, but they also select the bandwidths of these unstable modes. Further experiments using ternary mixtures with different compositions of PSC show that the bandwidths of unstable modes change with the conversion of the photodimerization of cinnamic acid ester moieties on the PSC chains. For high conversion, the PSC component accelerates the phase separation and consequently broadens the dispersion curve of the reacting mixture. Quantitative interpretation of these results cannot be obtained unless the set of coupled Cahn-Hilliard equations for reacting polymer mixtures is solved for these particular cross-link conditions.

### C. Morphology and phase separation kinetics of binary polymer mixtures (A/B) with reversible photoisomerization $A \rightleftharpoons B$

Recently, analytical calculation<sup>26</sup> and computer simulation<sup>16–19</sup> have predicted that the morphologies developing during the spinodal decomposition process of a reacting binary mixture (A/B) can be spontaneously frozen in the presence of the reversible reaction  $A \rightleftharpoons B$ . The prediction for the soft-modes suppression was derived for the first time by Huberman for the phase separation driven by autocatalytic reactions<sup>29</sup> and later by others for heterogeneous reactions on a catalytic surface.<sup>30</sup> From the viewpoints of materials science, it is critically important to verify this suppression process because this concept might provide very useful techniques to control the morphology of polymer mixtures by using reversible chemical reactions. For this purpose, *trans*-stilbene labeled polystyrene/poly(vinyl methyl ether) (PSS/PVME) mixtures were used as a model system. As mentioned early, upon irradiation with uv light, stilbene moieties on the PSS chains undergo reversible *trans*  $\leftrightarrow$  *cis* photoisomerization, inducing phase separation. The destabilization of PSS/PVME blends induced by this reaction was directly observed by light scattering<sup>31</sup> as well as by small-angle neutron scattering<sup>32</sup> from the sample before and after irradiation. The rates of the forward *trans*  $\rightarrow$  *cis* and the backward *cis*  $\rightarrow$  *trans* reactions can be adjusted by varying the excitation wavelength and the light intensity. Figure 11 shows the time

evolution of a PSS/PVME (50/50) blend irradiated by 365 nm uv light with the intensity  $4.1 \text{ mW/cm}^2$  at  $105^\circ\text{C}$ . The phase separation becomes observable under phase-contrast optical microscope after 20 min of irradiation. The morphology is an isotropic modulated structure with the characteristic length scale  $1.8 \mu\text{m}$  and is almost unchanged with irradiation time. However, these structures suddenly grow when the exciting light was turned off at 150 min of irradiation. The time evolution of the phase separation in the dark follows the Lifshitz-Slyozov-Wagner (LSW) power law<sup>33,34</sup>  $\xi(t) \propto t^\alpha$  with  $\alpha$  approximately equal to  $\frac{1}{3}$ . Taking into account that the molar extinction coefficients ( $\epsilon$ ) of the two isomers *cis*- and *trans*-stilbenes are almost unchanged at 365 nm, the kinetic data shown in Fig. 11 clearly indicate that the soft modes in the irradiated mixture were suppressed by the reversible isomerization of stilbene. On the other hand, upon irradiation with 313 nm uv light, the excitation condition where the *trans*  $\rightarrow$  *cis* isomerization is predominant ( $\epsilon_{\text{trans}}/\epsilon_{\text{cis}} \approx 4.3$ ), the phase separation exhibits a universal behavior under the light intensity in the range  $0.1\text{--}4.1 \text{ mW/cm}^2$ . It was found that  $\xi$  is almost unchanged with irradiation time in the early stage and then increases with irradiation time, following the LSW power law with  $\alpha = \frac{1}{3}$ . Eventually,  $\xi$  approaches a stationary value. It is theoretically predicted that the phase separation of a binary mix-

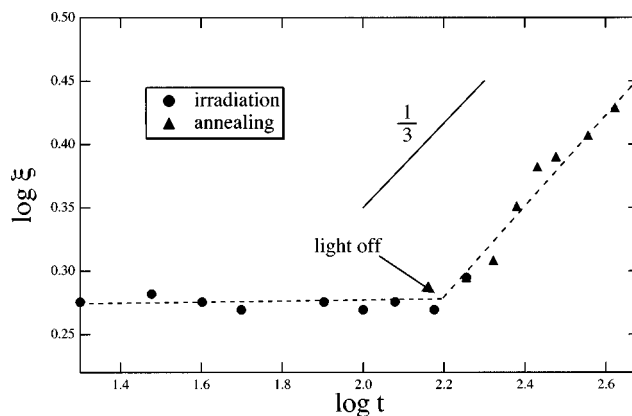


FIG. 11. Experimental evidence for the soft-mode suppression in a PSS/PVME (50/50) blend irradiated with 365 nm uv light at  $105^\circ\text{C}$ .

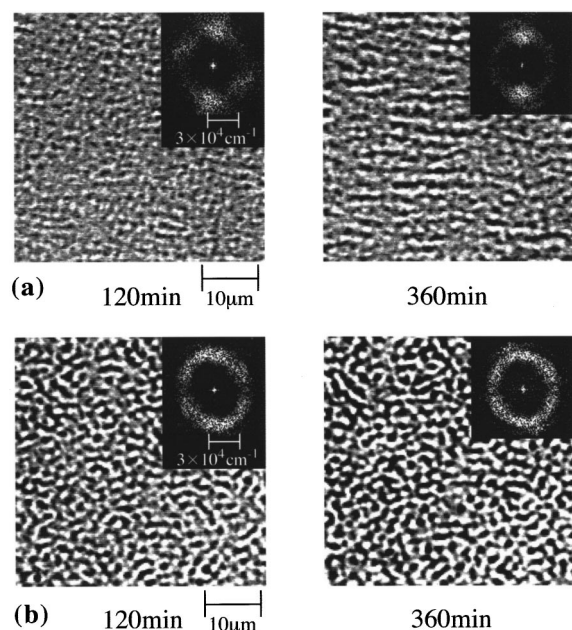


FIG. 12. Effects of annealing time on the morphology of a PSS/PVME (20/80) blend irradiated with 313 nm uv light ( $4.1 \text{ mW/cm}^2$ ) at  $90^\circ\text{C}$ : (a) without annealing; (b) with 30 min of annealing after each time of irradiation. The number below the micrograph indicates the duration of irradiation.

ture accompanied by a reversible reaction mathematically corresponds to the microphase separation of diblock copolymers<sup>4</sup> where the ratio of the reaction rate ( $k$ ) to the mobility ( $M$ ) of the former is mathematically equivalent to the inverse block-length ratio in the latter case. Therefore, predicts that by modifying the ratio  $k/M$ , a series of ordered structures such as hexagon, cylinder, lamellae and so on could be obtained, in principle, with reacting polymer mixtures. To examine this mathematical prediction, the above experiments were carried out with the irradiation intensity varying from 0.1 to  $4.1 \text{ mW/cm}^2$ . The average reaction rate  $k_0$  obtained by fitting the kinetic data to the KWW equation (16) varies from  $0.45 \times 10^{-2}$  to  $0.167 \text{ min}^{-1}$ . It was also found that, except for the case of the highest intensity  $4.1 \text{ mW/cm}^2$ , the morphology of the PSS/PVME (20/80) blend is isotropic. As shown in Fig. 12(a), the lamellar structure was obtained after 60 min of irradiation with 313 nm uv light ( $4.1 \text{ mW/cm}^2$ ). The anisotropy of the morphology of the irradiated blend becomes significant with increasing irradiation time. However, by annealing the blend over 30 min at the experimental temperature after each period of irradiation, the morphology becomes almost isotropic as seen in Fig. 12(b). From the inhomogeneous reaction kinetics and the irradiation-annealing experiments described above, it can be concluded that the lamellar structures emerging in the PSS/PVME (20/80) blend are originated from the couplings between the concentration fluctuations and the elastic stress associated with the reaction inhomogeneity, rather than from the mathematical equivalence with the microphase separation of block copolymers.

#### D. Remarks on the correlations between experimental data and current theoretical models for reaction-induced phase separation

From the viewpoint of theoretical modeling, as far as chemical reactions in the bulk state of polymers are concerned, the inhomogeneity of the reactions and the elastic stress associated with these structural changes should be taken into account. The approach using the time-dependent Ginzburg-Landau (TDGL) equation accompanied by a reversible reaction term<sup>16,26</sup> is suggestive and interesting because of the analogy with the microphase separation of diblock copolymers. The theoretical approach using the general concept of thermodynamics for reaction-diffusion systems suggests the existence of novel and important phenomena for chemically reacting mixtures: the Turing-like and the purely chemical instabilities.<sup>20</sup> However, these two theories are limited to systems of small molecules because the effects of elasticity, a long-range interaction, are not considered. In an attempt to explain the anisotropic morphology emerging from phase separation of binary metallic alloys, Onuki and Nishimori have taken into account the contribution of the elastic misfit between the two components to the kinetics of the spinodal decomposition.<sup>35</sup> On the other hand, the viscoelastic model of polymers based on the memories built-in by the cross-linking reactions<sup>22</sup> relies mainly on the mean-field kinetics. Though the viscoelasticity, a characteristic feature of polymers, was included in the model, the mean-field assumption for the reaction kinetics is not supported, in general, by the photo-cross-linking experiments. Particularly, the emergence of a positive feedback driven by reaction-induced fluctuations<sup>28</sup> was neglected in this viscoelastic model. There is also another important feature associated with the reaction inhomogeneity in polymer mixtures: the existence of the front of phase separation propagating from the position in the reacting mixture where the instability first takes place. This aspect has been analyzed recently by Furukawa who used the delta function as the initial condition for the order parameter in the Cahn-Hilliard equation.<sup>36</sup> The simulation reproduces the concentric (target) patterns observed by experiments.<sup>37</sup>

In order to completely understand the pattern formation process arising from the phase separation of chemically reacting polymer mixtures, it is currently necessary to build a theoretical model taking into account the mutual couplings among the reaction kinetics, thermodynamics and the viscoelasticity of the system.

#### V. CONCLUDING REMARKS AND PERSPECTIVES

(1) From the experimental results described above, it is obvious that unlike the nonreactive polymer mixtures, the phase separation in the presence of chemical reactions, particularly with reversible reactions, is unique. This process can lead to the formation of stationary structures with intrinsic length scales determined by the competition between antagonistic interactions: phase separation and reactions. These structures are known as modulated phases and have been observed over a wide range of materials.<sup>38,39</sup> Thus, the photodimerization and the photoisomerization shown here can be utilized as a “wave-

length selector'' for the unstable modes developing in the polymer mixtures under irradiation. On the other hand, the regularity of the morphology can be generated and controlled by breaking the spatial symmetry of the order parameter.

- (2) Since most chemical reactions proceed inhomogeneously in the bulk state of polymers,<sup>40</sup> the structural changes induced by chemical reactions in polymers are often accompanied by a gradient of elastic modulus. The successive couplings between the reaction and the elastic stress associated with these gradients can lead to a symmetry breaking of concentration fluctuations at the local scale whereby the spatial coherence emerges. By taking advantage of this unique property of polymeric materials, polymer blends with lamellar structures were obtained by cross-link with linearly polarized light.<sup>41</sup>
- (3) From the viewpoint of materials science, understanding the mode-selection and the spatial symmetry-breaking process induced by chemical reactions in binary polymer mixtures could provide useful and novel approaches for morphology control, a long-standing interest in materials science. With the matured knowledge acquired from the field of nonlinear dynamics, polymers with novel structures and functions could be designed and developed in the next decade.

## ACKNOWLEDGMENTS

This work was supported by the Ministry of Education, Science and Culture, Japan, through a Grant-in-Aid No. 09650998. The technical assistance of Asuka Harada (Dai-Nippon Ink and Chemicals Inc., Osaka), Katsunari Kataoka (Dai Nippon Printing Inc., Kyoto) and Takashi Ohta (Dynic Corp., Saitama) is greatly appreciated.

<sup>1</sup>See, for example, I. C. Sanchez, "Polymer Phase Separation," in *The Encyclopedia of Physical Science and Technology* (Academic, New York, 1987), Vol. XI.

<sup>2</sup>For example, see *Structure and Properties of Multiphase Polymeric Materials*, edited by T. Araki, Q. Tran-Cong, and M. Shibayama (Marcel Dekker, New York, 1998).

<sup>3</sup>M. Szwarc, *Carbanions, Living Polymers and Electron-Transfer Processes* (Wiley, New York, 1968).

<sup>4</sup>Y. Matsushita, Chap. 4: *Block and Graft Copolymers*, in Ref. 2, pp. 121–154.

<sup>5</sup>See, for example, A. Echte, in *Rubber-Toughened Plastics*, edited by C. Keith Riew, Adv. Chem. Ser. No. 222 (American Chemical Society, Washington, DC, 1989), pp. 15–64.

<sup>6</sup>A. I. Nakatani and C. C. Han, Chap. 7: *Shear Dependence of the Equilibrium and Kinetic Behavior of Multicomponent Systems*, in Ref. 2, pp. 233–267.

<sup>7</sup>For example, see M. C. Cross and P. C. Hohenberg, *Rev. Mod. Phys.* **65**, 851 (1993).

<sup>8</sup>C. Vidal, G. Dewel, and P. Borckmans, *Au-delà de L'équilibre* (Hermann, Paris, 1994).

<sup>9</sup>*Principles of Solidification and Materials Processing*, edited by R. Trivedi, J. A. Sekhar and J. Mazumdar (Trans Tech Publications, Switzerland, 1991), Vols. 1 and 2.

<sup>10</sup>*Nonlinear Phenomena in Materials Science*, edited by L. P. Kubin and G. Martin (Trans Tech Publications, Switzerland, 1987), Vol. I.

<sup>11</sup>G. Nicolis and I. Prigogine, *Self-Organization in Nonequilibrium Systems* (Wiley, New York, 1977).

<sup>12</sup>J. P. Flory, *Principle of Polymer Chemistry* (Cornell U.P., Ithaca, 1953), Chaps. 12 and 13.

<sup>13</sup>J. W. Cahn and J. E. Hilliard, *J. Chem. Phys.* **28**, 258 (1958).

<sup>14</sup>K. Binder, *Adv. Polym. Sci.* **112**, 181 (1994).

<sup>15</sup>P.-G. de Gennes, *J. Chem. Phys.* **72**, 4756 (1980).

<sup>16</sup>S. C. Glotzer, E. A. Di Marzio, and M. Muthukumar, *Phys. Rev. Lett.* **74**, 2034 (1995); S. C. Glotzer, in *Annual Reviews of Computational Physics*, edited by D. Stauffer (World Scientific, Singapore, 1995), Vol. 2, pp. 1–46.

<sup>17</sup>J. J. Christensen, K. Elder, and H. C. Fogedby, *Phys. Rev. E* **54**, 2212 (1996).

<sup>18</sup>M. Motoyama, *J. Phys. Soc. Jpn.* **65**, 1894 (1997).

<sup>19</sup>S. Toxvaerd, *Phys. Rev. E* **53**, 3710 (1996).

<sup>20</sup>D. Carati and R. Lefever, *Phys. Rev. E* **56**, 3127 (1997).

<sup>21</sup>A. Imagawa and Q. Tran-Cong, *Macromolecules* **28**, 8388 (1995); T. Tamai, A. Imagawa and Q. Tran-Cong, *ibid.* **27**, 7486 (1994).

<sup>22</sup>H. Nakazawa and K. Sekimoto, *J. Chem. Phys.* **104**, 1675 (1996).

<sup>23</sup>J. J. McCullough, *Chem. Rev.* **87**, 811 (1987).

<sup>24</sup>J. Saltiel, J. D'Agostino, E. D. Megarity, L. Metts, K. R. Neuberger, M. Wrighton, and O. C. Zafiriou, in *Organic Photochemistry*, edited by O. L. Chapman (Marcel Dekker, New York, 1973), Vol. 3, pp. 1–113.

<sup>25</sup>A. Harada and Q. Tran-Cong, *Macromolecules* **30**, 1643 (1997).

<sup>26</sup>S. C. Glotzer and A. Coniglio, *Phys. Rev. E* **50**, 4241 (1994).

<sup>27</sup>G. Williams and D. C. Watts, *Trans. Faraday Soc.* **66**, 80 (1970).

<sup>28</sup>Q. Tran-Cong, A. Harada, K. Kataoka, T. Ohta, and O. Urakawa, *Phys. Rev. E* **55**, R6340 (1997).

<sup>29</sup>B. A. Huberman, *J. Chem. Phys.* **65**, 2013 (1976).

<sup>30</sup>J. Verdasca, P. Borckmans, and G. Dewel, *Phys. Rev. E* **52**, 4616 (1995).

<sup>31</sup>Q. Tran-Cong, T. Ohta and O. Urakawa, *Phys. Rev. E* **56**, R59 (1997).

<sup>32</sup>O. Urakawa, O. Yano, Q. Tran-Cong, A. I. Nakatani, and C. C. Han, *Macromolecules* **31**, 7962 (1998).

<sup>33</sup>I. M. Lifshitz and V. V. Slyozov, *J. Phys. Chem. Solids* **19**, 35 (1961).

<sup>34</sup>C. Z. Wagner, *Z. Elektrochem.* **65**, 581 (1961).

<sup>35</sup>A. Onuki and H. Nishimori, *Phys. Rev. B* **43**, 13649 (1991).

<sup>36</sup>H. Furukawa, *J. Phys. Soc. Jpn.* **63**, 3744 (1994); **63**, 3919 (1994).

<sup>37</sup>Q. Tran-Cong and A. Harada, *Phys. Rev. Lett.* **76**, 1162 (1996).

<sup>38</sup>M. Seul and D. Andelman, *Science* **267**, 476 (1995).

<sup>39</sup>C. Roland and R. C. Desai, *Phys. Rev. B* **42**, 6658 (1990).

<sup>40</sup>K. Kataoka, A. Harada, T. Tamai, and Q. Tran-Cong, *J. Polym. Sci., Part B: Polym. Phys.* **36**, 455 (1998).

<sup>41</sup>Q. Tran-Cong, K. Kataoka, and O. Urakawa, *Phys. Rev. E* **57**, R1243 (1998).